

Selected Paper

Blue Phosphorescence of the Novel Dinuclear Gold(I) Complex Bridged by 1,3-Benzenedithiolate in Solution

Seiji Watase, Takayuki Kitamura,[1] Yasuchika Hasegawa,[1] Nobuko Kanehisa,[2] Masami Nakamoto, Yasushi Kai,[2] and Shozo Yanagida*[,1]

Osaka Municipal Technical Research Institute, 1-6-50 Morinomiya, Joto-ku, Osaka 536-8553

[1]Material and Life Science, Graduate School of Engineering, Osaka University, 2-1 Yamadaoka, Suita, Osaka 565-0871

[2]Department of Materials Chemistry, Graduate School of Engineering, Osaka University, 2-1 Yamadaoka, Suita, Osaka 565-0871

Received September 26, 2003; E-mail: yanagida@mls.eng.osaka-u.ac.jp

A novel dinuclear benzenedithiolatogold(I) complex was synthesized and characterized spectroscopically. This complex showed intense blue emission [quantum yield at 1.0×10^{-4} mol dm^{-3}: $\Phi = 0.026(2)$] at room temperature in fluid solvents. This emission originates from a metal-perturbed ligand-centered transition. The relatively long life time of the excited state (τ_{50} = ca. 2 μsec) and the large stokes shift suggest that the emission is phosphorescence. The X-ray single crystal structural determination showed that the complex has a distorted 12-membered macrocyclic structure bridged by two benzenedithiolate ligands, with no gold–gold interactions.

Photoluminescent properties of gold(I) complexes in both solid state and solution have attracted much attention over the past decade because of potential applications, such as luminescence-based sensors for oxygen,[1] alkali ions,[2] or volatile organic compounds,[3] and electroluminescence devices.[4–6] The luminescence of gold(I) complexes has been significantly related to the gold–gold interactions induced by relativistic effects. However, some mononuclear thiolatogold(I) complexes, [Au(PPh$_3$)(SPh)],[7] [Au(tpa)SPh] (tpa = 1,3,5-triaza-7-phosphaadamantanetriylphosphine),[7] and (n-Bu$_4$N)[Au(SPh)$_2$][8,9] and a dinuclear gold(I) complex, [Au$_2$(dppe)(SR)$_2$] (dppe = diphenylphosphinoethane; R = C$_6$H$_5$-p-Me),[10] show luminescence in the solid state even without such aurophilic interactions. Therefore, solid-state luminescence can be qualified as one of the characteristic properties of thiolatogold(I) complexes regardless of the gold–gold interaction.

On the other hand, luminescent behavior in solution has different aspects from the solid-state luminescence. Many thiolatogold(I) complexes with the intramolecular gold–gold interaction show luminescence in solution,[2,3,11–14] but the luminescence of thiolatogold(I) complexes with no gold–gold interaction has rarely been reported. While a dimeric gold(I) complex [Au(S-2-pym-4,6-Me$_2$)]$_2$ (pym = pyrimidine) with an intramolecular gold–gold interaction shows luminescence both in fluid solutions and in 95 K frozen glasses, the monomeric [Au(S-2-pym-4,6-Me$_2$)(S-2-pymH-4,6-Me$_2$)] (pymH = pyrimidinium) obtained by the degradation of [Au(S-2-pym-4,6-Me$_2$)]$_2$ is nonemissive at room temperature in fluid solution.[15] Another mononuclear gold(I) complex with 2-pyridinethiolate and diphenyl-2-pyridylphosphine ligands, [Au(S-2-py)(PPh$_2$py)] (py = pyridine), shows extremely weak emission at room temperature in solution.[16] However, in acidic solution, the dinuclear complex, [{Au(S-2-pyH)(PPh$_2$py)}$_2$](PF$_6$)$_2$ (pyH = pyridinium), formed by self-association through N–H···N type hydrogen bonds and by gold–gold interaction showed increased luminescence. These results indicate that the thiolatogold(I) complexes, even in mononuclear complexes, show luminescence in fluid solution under the conditions to form gold–gold interaction and to increase the environmental rigidity because such interactions can serve effectively as the structural restraints.

In another case, open-ring dinuclear gold(I) complexes with bidentate phosphine ligand having small bite angles, [Au$_2$-{Ph$_2$PN(R)PPh$_2$}(SR)$_2$] (R = Ph, cyclohexyl, i-Pr)[17] and [1,3-C$_6$H$_4$(OPPh$_2$AuSPh)$_2$][18] are also emissive in fluid media, because free rotation of ligand moieties is restricted by structurally imposed steric restraints. In other words, the introduction of the structural restraint to the molecular system is a primary condition to gain the luminescence of the gold(I) complexes in solution. Therefore, the introduction of a closed-ring structure through ligands into the molecular system must be one of the effective strategies to obtain the luminescence in room temperature fluid solution regardless of gold–gold interaction.

Previously, we reported relatively strong emission from mononuclear benzenethiolatogold(I) complexes (Scheme 1) in the solid state at room temperature, where intermolecular

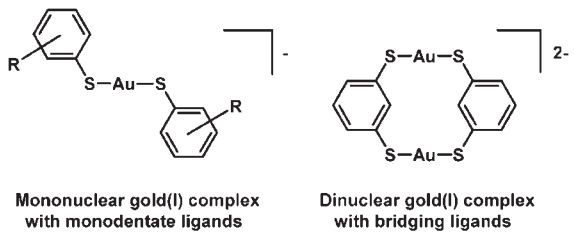

Scheme 1.

Published on the web March 12, 2004; DOI 10.1246/bcsj.77.531

gold–gold interaction is completely inhibited by using bulky tetra-*n*-butylammonium as the counter cation.[8,9] However, these complexes show quite weak emission in organic solution because of the vibrational quenching caused by the free-rotation of thiolate ligands, owing to their linear two-coordination geometry with less structural restraint. To obtain the strong emission from thiolatogold(I) complexes without gold–gold interaction in fluid solution at room temperature, we designed a novel dinuclear gold(I) complex with 1,3-benzenedithiolate as a bridging ligand; the resulting macrocyclic complex could have a rigid structure due to restricted rotation at the Au–S and the S–C bonds and the two gold centers could be located separately from each other, giving no intra- and intermolecular gold–gold interactions (Scheme 1). In this report, we describe the luminescent behavior of the novel dinuclear bis(benzenedithiolate)digold(I) complex, $(n\text{-}Bu_4N)_2[Au_2(S_2\text{-}1,3\text{-}C_6H_4)_2]$ (**1**) in fluid solution.

Results and Discussion

Spectroscopy. Electronic absorption spectra of the present complex **1** were measured in several organic solvents, including acetonitrile, acetone, dichloromethane, tetrahydrofuran, and toluene. The representative absorption spectrum in acetonitrile is depicted in Fig. 1 together with excitation and emission spectra in the same solvent. Absorption band positions and extinction coefficients in all solvents are summarized in Table 1 together with emission maxima. The absorption spectrum in acetonitrile displayed intense absorption bands in the ultraviolet region having a peak maximum at 274 nm (ε, 36000 mol^{-1} dm^3 cm^{-1}) with a shoulder at 304 nm (ε, 16000 mol^{-1} dm^3 cm^{-1}). The relatively weak absorption bands were also found in the range of 320–360 nm, and two weak bands were determined by the second derivative curve of the spectrum at 326 (ε, 5200 mol^{-1} dm^3 cm^{-1}) and 337 nm (ε, 2800 mol^{-1} dm^3 cm^{-1}), respectively. The absorption spectra in each solvent were nearly identical in shape and the extinction coefficients were close to each other. Furthermore, negligible shift of the spectra was observed in spite of different solvent polarity values.

The assignments of absorption bands in the ultraviolet region of the gold(I) complexes containing benzenethiolate ligands are very complicated, because various transitions, such as metal-centered (MC), ligand-centered (LC), ligand-to-metal charge-transfer (LMCT), or metal-to-ligand charge-transfer (MLCT) transitions, could exist in the same region.[11,12,14,19] In the case of phosphine thiolatogold(I) complexes, the most intense absorption band in this region was assigned to LMCT transition.[20] However, mixing of the π–π^* transitions in the benzenethiolate ligands in this region cannot be ruled out, because these transitions of the benzenethiolate ligands of these gold(I) complexes were also observed in the same region.[20] In the present complex, the gold center may have more electron-rich circumstances than those of phosphine thiolatogold(I) complexes because of dual coordination of the donating dithiolate ligand, similar to the reported mononuclear bis(benzenethiolato)gold(I) complexes.[8,9] Such coordination would result in the elevation of metal orbitals Au 5d and Au 6p (Scheme 2). The elevation of Au 6p level, in consequence of donation from the dithiolates, could make the π^* orbital an acceptor orbital. On the other hand, the elevated Au 5d orbitals act as a counterbalance to non-bonding orbitals, S(n). Thus, the absorption bands observed at 274 and 304 nm may be assigned to MLCT and/or LC transition perturbed by the heavy gold atom. Low lying absorption bands at 326 and 337 nm were tentatively assigned to spin-forbidden singlet to triplet, $S_0 \rightarrow T$, transitions induced by the heavy atom effect of gold.[21] The excitation spectrum is in good agreement with the corresponding absortion spectra as shown in Fig. 1. This complex showed an intense blue emission with excitation at 274 nm in several degassed organic solvents at room temperature. The peak maximum of this blue emission was observed at 437 nm in acetonitrile and the maxima in other solvents lay in almost the same positions (Table 1). A large separation (13600 cm^{-1}) between absorption and emission spectra, and the emission quenching behavior in the presence of the oxygen strongly suggest that the emission is phosphorescence.

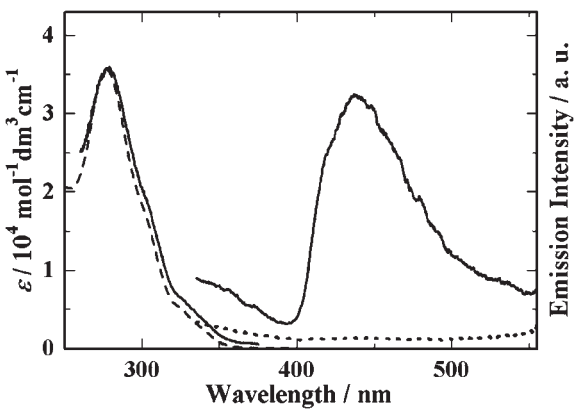

Fig. 1. Representative absorption (broken line), excitation ($\lambda_{em} = 437$ nm), and emission ($\lambda_{ex} = 285$ nm) spectra of complex **1** in acetonitrile (5×10^{-6} mol dm^{-3}) at room temperature. Dotted line shows emission spectrum of **1** ($\lambda_{ex} = 285$ nm) in the presence of oxygen.

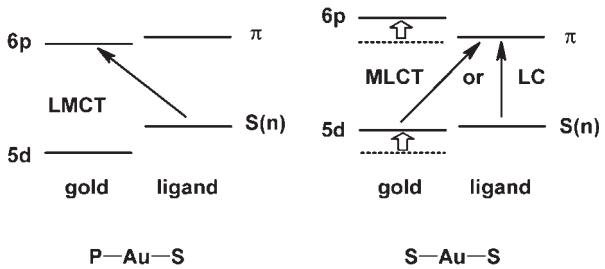

Scheme 2. Schematic representation of possible transitions.

Table 1. Spectroscopic Data for Complex **1**

Solvent	λ_{abs}/nm (ε/mol^{-1} dm^3 cm^{-1})				λ_{em}/nm
acetonitrile	274 (36000)	304 (16000)	326 (5200)	337 (2800)	437
acetone	—	—	—	339 (2900)	437
dichloromethane	276 (32000)	303 (17000)	327 (5200)	339 (2600)	438
tetrahydrofuran	—	305 (18000)	328 (4800)	340 (2700)	440
toluene	—	304 (17000)	328 (5100)	340 (2900)	441

This blue emission was also observed with excitation in the region of the low lying absorption bands. In addition, a relatively weak emission band was also detected in the same region of the low-lying absorption bands with excitation at 274 nm, this was obscure owing to an interruption of the solvent Raman peak. However, quenching behavior by the oxygen suggests that this weak emission can be assigned to phosphorescence and may be due to the higher triplet excited states, T_n. Thus, the low-lying absorption bands in the range of 300–360 nm may be responsible for direct transitions from ground state to higher triplet excited states, T_n, accompanied with the internal conversion from T_n to T_1 excited state, giving the blue phosphorescence. Insensitivity to the solvent polarity of the emission spectrum suggests that any CT-type transition should be ruled out as a potential emission origin. Therefore, we concluded that the emission origin of the complex **1** could be assigned to the metal-perturbed triplet ligand-centered transition, ^{3}LC [S(n) $\leftarrow \pi^*$].

Emission Quantum Yield and Life Time. The measurements of emission quantum yield and emission lifetime at 355 nm of this complex were carried out using toluene solution. The results show relatively higher emission intensity than in other solvents. Emission quantum yield measurements were conducted for several low concentrations, 1.0×10^{-4}, 1.9×10^{-4}, 3.2×10^{-4}, and 4.0×10^{-4} mol dm^{-3} of toluene solutions, which were used after the filtration and degassing process was conducted in five freeze–pump–thaw cycles. Emission quantum yield decreased with increase of concentration, showing the concentration-dependent quenching (Fig. 2). The plots of the inverse of the relative quantum yield ($1/\Phi$) versus solution concentrations gave a linear relationship. The least square linear fit is in good agreement with the plots over a limited range of the tested concentration range, similar to the Stern–Volmer type expression. This quenching may be caused by collisions of the molecules with each other in the excited states based on the diffusion control, showing self-quenching or T–T annihilation. Since the emission spectra in each concentration were identical in shape, the generation of the excimer can be excluded. Therefore, the T–T annihilation may be contributory despite low concentrations, but this conclusion is tentative at this moment. However, the quantum yield of this complex in toluene is 0.026(2) at 1.0×10^{-4} mol dm^{-3} and the quantum yield at infinite dilution (Φ^0) calculated by the interpolation of the least square fitting line of the plots is ca. 0.08. It is an extremely high quantum yield among thiolatogold(I) analogues.

The emission decay curve of the present complex in toluene (3.2×10^{-4} mol dm^{-3}) was obtained with excitation at 355 nm using Nd-YAG laser as shown in Fig. 3. In the case of the emission decay process containing the collision quenching processes, such as the T–T annihilation, the decay curve can not be analyzed by the single exponential fitting. Then the decay lifetime of the emission can be estimated as the period of half-decay of the emission intensity (Fig. 3). The relatively long half-decay τ_{50} of ca. 2 μsec in toluene also supports the conclusion that the emission is phosphorescence.

^{1}H-NMR Measurement. ^{1}H-NMR measurements were carried out using deuterated toluene and acetonitrile (Fig. 4). In toluene solution, the chemical shifts of the peaks assigned to H1 and H5 located in the inside of the 12-membered ring were observed at 8.89 ppm and showed slightly separated doublet-doublet signals by remote coupling with H2 and H4 or H6 and H8. The chemical shifts of H3 and H7 were observed at 6.83 ppm, showing two pairs of doublets due to the coupling with neighbouring protons, H2 and H4 or H6 and H8. The

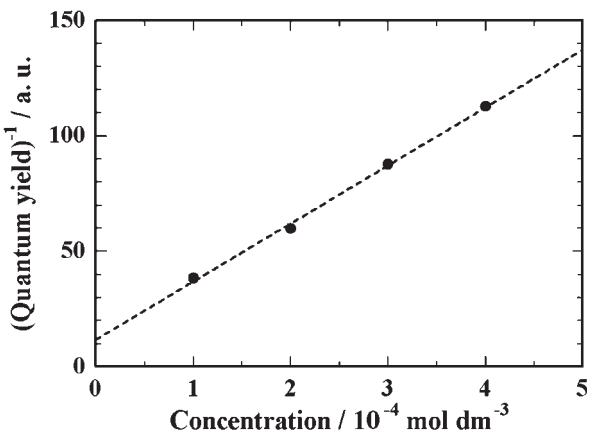

Fig. 2. Concentration-dependent emission quenching behavior of complex **1** in toluene.

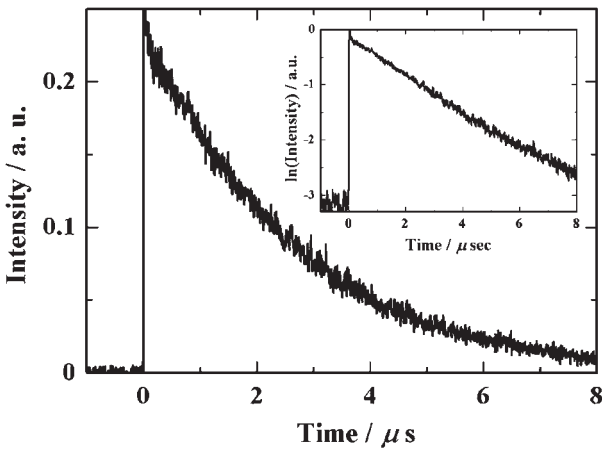

Fig. 3. Emission decay curve of complex **1** in toluene (3.2×10^{-4} mol dm^{-3}). Inset shows the plot of logarithm of the intensity versus time.

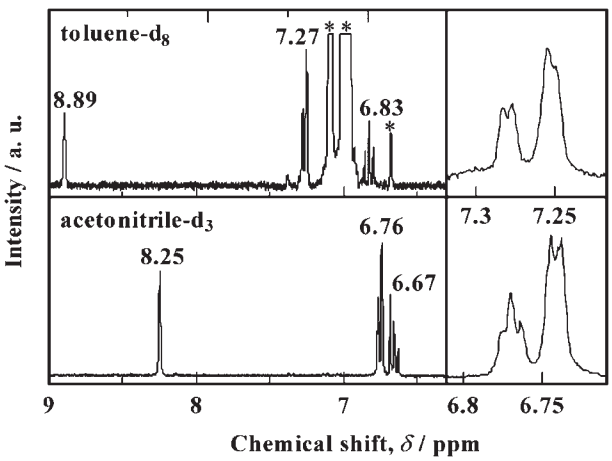

Fig. 4. ^{1}H-NMR spectra of the aromatic region of complex **1** in toluene-d_8 (top) and in acetonitrile-d_3 (bottom) with magnifications (right). * solvent.

peaks of H2, H4, H6, and H8 observed at 7.27 ppm were too complicated to identify. There were two pairs of doublet-doublet signals, but they have slightly different separations and positions, giving asymmetric shaped peaks. In the case of acetonitrile solution, all peaks assigned to aromatic protons (H1–H8) were shifted toward higher magnetic field than those in toluene solution, owing to the solvent polarity of acetonitrile being higher than that of toluene. The peaks of H1 and H5 shifted 0.64 ppm and were observed at 8.25 ppm. H2 and H7 signals positioned at 6.67 ppm also showed the doublet-doublet coupling. The remaining protons: H2, H4, H6, and H8 still had an asymmetric feature and were detected around 6.76 ppm. Thus, these results suggest that two phenyl rings of the complex anion have slightly different circumstances due to the distorted ligand conformations. Therefore this complex probably maintained the asymmetric structures similar to those in crystal even in both toluene and acetonitrile solution, at least over the time scale of the NMR measurements (vide infra).

Crystal Structure. The single crystal of the present complex obtained from methanol was suitable for the X-ray analysis. Crystallographic data are all compiled in Table 2. Selected bond distances and angles are listed in Table 3. The complex **1** crystallized in the monoclinic space group $P2_1/c$ (No. 14). The perspective drawing[22] of complex anion of **1** is depicted in Fig. 5. The complex **1** has a twisted 12-membered ring structure, but no guest is included in the ring. Each of the gold centers has linear two-coordinate geometry with bridging dithiolate ligands. The S1–Au1–S3 and the S2–Au2–S4 moieties deviate slightly from the linearity (Fig. 5 and Table 3) and they are not parallel to each other. The intramolecular Au···Au separation of 5.181(1) Å is indicative of negligible gold–gold interaction. Four Au–S–C angles are slightly smaller than those of the related mononuclear complexes [108.4(1)–111.8(8)°],[8,9] but the Au2–S4–C9 angle is quite smaller than the others. The dihedral angle between two phenyl rings of 127.2(4)° reveals that the structure of this complex anion largely deviated from the planarity. These structural details clearly indicate that the present complex has an asymmetric structure in the crystal. This result is consistent with the ^{1}H-NMR measurements in solution, as described above. Two bulky counter cations, $(n\text{-}Bu_4N)^+$ are placed around the complex anions, and these apparently prevent intermolecular gold–gold interaction in the solid state. The closest intermolecular interatomic Au···Au distance of 8.730(1) Å in the solid state excludes the presence of any intermolecular interaction. A similar structure may be operative in solution.

Table 2. Crystallographic Data for Complex **1**

Crystal params	Complex **1**
Empirical formula	$C_{44}H_{80}N_2S_4Au_2$
Formula weight	1159.30
Crystal system	monoclinic
Space group (No.)	$P2_1/c$ (#14)
Z	4
a/Å	16.6266(5)
b/Å	14.2750(3)
c/Å	21.3841(6)
α/deg	90.00
β/deg	91.1483(8)
γ/deg	90.00
Volume/Å^3	5074.4(2)
ρ_{calcd}/g cm^{-3}	1.517
Crystal dimension/mm^3	0.13 × 0.12 × 0.10
Temperature/K	296
Radiation	Mo, 0.71069
F(000)	2320
Independent reflections [R_{int}]	11437 [0.049]
No. of observed data	4701 ($I < 2.0\sigma(I)$)
No. of parameters varied	469
μ/cm^{-1}	59.89
$R1$[a)], Rw[b)]	0.042, 0.066

a) $R1 = \Sigma||Fo| - |Fc||/\Sigma|Fo|$. b) $Rw = (\Sigma w(Fo^2 - Fc^2)^2/\Sigma w(Fo^2)^2)^{1/2}$.

Table 3. Selected Bond Distances (Å) and Angles (deg) for Complex **1**

Au1–S1	2.283(3)	Au1–S3	2.275(3)
Au2–S2	2.273(3)	Au2–S4	2.277(3)
S1–C1	1.78(1)	S3–C7	1.77(1)
S2–C3	1.76(1)	S4–C9	1.78(1)
S1–Au1–S3	178.1(1)	S2–Au2–S4	179.2(1)
Au1–S1–C1	106.1(3)	Au1–S3–C7	106.4(4)
Au2–S2–C3	106.4(3)	Au2–S4–C9	100.1(3)
Au1–Au2[a)]	5.1814(5)	Au1···Au1[b)]	8.9828(5)
Au2···Au2[b)]	8.7298(4)	Au1···Au2[b)]	8.7763(6)
C1plane–C7plane[c)]	127.3(5)		

a) Intramolecular interatomic distance. b) Intermolecular interatomic distances. c) Dihedral angle.

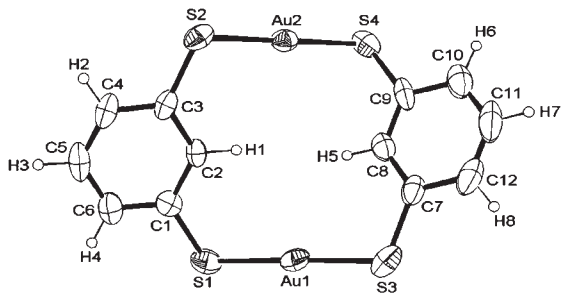

Fig. 5. Perspective view of the anion of complex **1** with the atomic numbering scheme crystallized from methanol solution. Thermal ellipsoids are drawn at the 30% probability level.

Conclusion

A novel dinuclear gold(I) complex with 1,3-benzendithiolate was synthesized and characterized spectroscopically and structurally. This dinuclear gold(I) complex with structural inflexibility resulting form the bridged dithiolate ligands showed an intense blue phosphorescence at room temperature in fluid solution, despite the absence of gold–gold interactions. The emission quantum yield (Φ) was 0.026(2) at 1.0×10^{-4} mol dm^{-3} of room temperature toluene solution, despite the absence of gold–gold interactions. This result strongly suggests that the environmental rigidity plays an important role in the improvement of the luminescence properties of the gold compounds in fluid media.

Experimental

Chemicals. Commercially available tetrachloroauric acid, $HAuCl_4 \cdot 4H_2O$, and benzenedithiol, C_6H_4-1,3-$(SH)_2$ were used without further purification. Triethylamine was purified by distillation. Tetrahydrofuran (THF) as a reaction solvent was distilled over CaH_2 under a nitrogen atmosphere before use. Spectroscopic grade solvents are received from Nacalai tesque. Tetra-*n*-butylammonium dibromoaurate(I), (n-Bu_4N)[$AuBr_2$], was prepared by the literature method.[23]

Synthesis. (n-Bu_4N)$_2$[Au_2(S_2-1,3-C_6H_4)$_2$] (**1**). The present complex was synthesized by the following Eq. 1. A mixture of 1,3-benzenedithiol (0.37 g, 3.3 mmol) and triethylamine (0.34 g, 3.3 mmol) in THF (20 cm^3) was added dropwise to a solution of (n-Bu_4N)[$AuBr_2$] (1.00 g, 1.7 mmol) in the same solvent (10 cm^3) and this combination was stirred for 3 h at room temperature. The white precipitate of Et_3NHBr was filtered off and the THF was evaporated under reduced pressure to give white residue stoichiometrically. The white residue was triturated with diethyl ether (3 cm^3) two times and the solvent was removed, and then the residue was dried in vacuo. The product was purified by recrystallization from methanol to give colorless crystals of complex **1** suitable for single-crystal X-ray analysis in 80% yield. Anal. Calcd for $C_{44}H_{80}N_2S_4Au_2$: C, 45.59; H, 6.96; N, 2.42%. Found: C, 45.36; H, 7.17; N, 2.42%.

$$2(n\text{-}Bu_4N)[AuBr_2] + 2C_6H_4\text{-}1,3\text{-}(SH)_2 + 4Et_3N \rightarrow (n\text{-}Bu_4N)_2[Au_2(S_2\text{-}1,3\text{-}C_6H_4)_2] + 4Et_3NHBr. \quad (1)$$

Instrumentation. Elemental analysis was performed on a CE Instruments EA 1110 Elemental Analyzer. ^{1}H-NMR spectra were collected on a JEOL JNM-EX270 Spectrometer and the chemical shifts were relative to the signal of tetramethylsilane (TMS) as an internal standard.

Optical Measurements. UV–visible absorption spectra were recorded on a Shimadzu UV-3100 spectrophotometer. Emission and excitation spectra were measured at room temperature with a Hitachi F-4500 system using a Xenon lamp as the excitation source. Spectra were corrected for instrumental response. Quantum yields of emission were determined using a standard integrating sphere (diameter 6 cm) according to the literature method.[24] The optical path length of the quartz cell was 5 mm. Corrected intensity function of excitation [$I_{ex}(\lambda_{ex})$: without a sample] was determined by the excitation spectrum of the system [$g_{ref}(\lambda)$: without a sample, 340–370 nm, scan rate = 240 nm/min].

$$I_{ex}(\lambda_{ref}) = \frac{\phi}{\int g_{ref}(\lambda)\mathrm{d}\lambda} g_{ref}(\lambda). \quad (2)$$

In Eqs. 2 and 3, ϕ is the light intensity of excitation. The corrected intensity function of light absorption with sample, $I_{ex}(\lambda_{sam})$, was also determined from the excitation spectra of the system (340–370 nm, scan rate = 240 nm/min), whereas the corrected intensity function of the emission was determined from the emission spectrum [$I_{em}(\lambda)$, 360–700 nm, scan rate = 240 nm/min]. The quantum yield, Φ, was calculated from Eq. 3:

$$\Phi = \frac{N_{emission}}{N_{absorption}} = \frac{\int \frac{\lambda}{hc} I_{em}(\lambda)\mathrm{d}\lambda}{\int \frac{\lambda}{hc}\{I_{ex}(\lambda_{ex}) - I_{ex}(\lambda_{sam})\}\mathrm{d}\lambda}. \quad (3)$$

The quantum yield of Rhodamine 6G in methanol (Ex at 488 nm, 510–760 nm, emission quantum yield = 95 ± 3%) determined by the present procedure agreed well with reported values. Solutions filtrated by a membrane filter were degassed with no fewer than five freeze–pump–thaw cycles. The emission signals were obtained at room temperature using the 355 nm third harmonic of a Q-switched Nd:YAG laser (Spectra Physics, INDI-50, fwhm = 5 ns, λ = 1064 nm) and a photomultiplier (Hamamatsu photonics, R7400U-03, response time $\leq$ 0.78 ns). Emission from the sample was monochromated by a Shimadzu SPG-100ST placed in front of the detector. Nd:YAG response was monitored with a digital oscilloscope (Sony Tektronix, TDS3052, 500 MHz) synchronized to the single pulse excitation.

Crystallography. The colourless single crystal of the complex **1** was obtained by recrystallization. This single crystal was mounted on glass fibres with epoxy resin. Intensity data were collected at room temperature on a Rigaku RAXIS-RAPID imaging-plate diffractomater with graphite-monochromated Mo-Kα radiation and the ω scan mode. The camera radius was 127.40 mm. Readout was performed in the 0.100 mm pixel mode. The data were collected at room temperature to a maximum 2θ value of 55.0°. Data were processed by the PROCESS-AUTO[25] program package. A symmetry-related absorption correction was applied using the program ABSCOR.[26] The data were corrected for Lorentz and polarization effects. The structures were solved by direct methods[27] and expanded using Fourier technique.[28] The non-hydrogen atoms were refined anisotropically. Hydrogen atoms were placed in calculated positions (C–H = 0.95 Å) but not refined. The final cycle of full-matrix least-squares refinement was based on observed reflections and variable parameters. All calculations were performed using the TEXSAN[29] crystallographic software package of Molecular Structure Corporation.

References

1 A. Mills, A. Lepre, B. R. C. Theobald, E. Slade, and B. A. Murrer, *Anal. Chem.*, **69**, 2842 (1997).

2 V. W.-W. Yam, C.-K. Li, and C.-L. Chan, *Angew. Chem., Int. Ed.*, **37**, 2857 (1998).

3 M. A. Mansour, W. B. Connick, R. J. Lachicotte, H. J. Gysling, and R. Eisenberg, *J. Am. Chem. Soc.*, **120**, 1329 (1998).

4 Y. Ma, C.-M. Che, H.-Y. Chao, X. Zhou, W.-H. Chau, and J. Shen, *Adv. Mater.*, **11**, 852 (1999).

5 Y. Ma, X. Zhou, J. Shen, H.-Y. Chao, and C.-M. Che, *Appl. Phys. Lett.*, **74**, 1361 (1999).

6 V. W.-W. Yam, C.-L. Chan, S. W.-K. Choi, K. M.-C. Wong, E. C.-C. Cheng, S.-C. Yu, P.-K. Ng, W.-K. Chan, and K.-K. Cheung, *Chem. Commun.*, **2000**, 53.

7 J. M. Forward, D. Bohmann, J. P. Fackler, Jr., and R. J. Staples, *Inorg. Chem.*, **34**, 6330 (1995).

8 S. Watase, M. Nakamoto, T. Kitamura, N. Kanehisa, Y. Kai, and S. Yanagida, *J. Chem. Soc., Dalton Trans.*, **2000**, 3585.

9 S. Watase, T. Kitamura, N. Kanehisa, M. Nakamoto, Y. Kai, and S. Yanagida, *Chem. Lett.*, **32**, 1002 (2003).

10 W. B. Jones, J. Yuan, R. Narayanaswamy, M. A. Young, R. C. Elder, A. E. Bruce, and M. R. M. Bruce, *Inorg. Chem.*, **34**, 1996 (1995).

11 S. S. Tang, C.-P. Chang, I. J. B. Lin, L.-S. Liou, and J.-C. Wang, *Inorg. Chem.*, **36**, 2294 (1997).

12 Y.-A. Lee, J. E. McGarrah, R. J. Lachicotte, and R. Eisenberg, *J. Am. Chem. Soc.*, **124**, 10662 (2002).

13 B.-C. Tzeng, C.-K. Chan, K.-K. Cheung, C.-M. Che, and

S.-M. Peng, *Chem. Commun.*, **1997**, 135.

14 B.-C. Tzeng, C.-M. Che, and S.-M. Peng, *Chem. Commun.*, **1997**, 1771.

15 L. Hao, R. J. Lachicotte, H. J. Gysling, and R. Eisenberg, *Inorg. Chem.*, **38**, 4616 (1999).

16 L. Hao, M. A. Mansour, R. J. Lachicotte, H. J. Gysling, and R. Eisenberg, *Inorg. Chem.*, **39**, 5520 (2000).

17 V. W.-W. Yam and C.-L. Chan, *J. Chem. Soc., Dalton Trans.*, **1996**, 4019.

18 W. J. Hunks, M. C. Jennings, and R. J. Puddephatt, *Inorg. Chem.*, **39**, 2699 (2000).

19 A. Vogler and H. Kunkely, "Transition Metal and Rare Earth Compounds," ed by H. Yersin, Springer, Berlin (2001), Vol. 213, p. 143.

20 R. Narayanaswamy, M. A. Young, E. Parkhurst, M. Ouellette, M. E. Kerr, D. M. Ho, R. C. Elder, A. E. Bruce, and M. R. M. Bruce, *Inorg. Chem.*, **32**, 2506 (1993).

21 L. J. Larson, E. M. McCauley, B. Weissbart, and D. S. Tinti, *J. Phys. Chem.*, **99**, 7218 (1995).

22 ORTEP-3; L. J. Farrugia, *J. Appl. Cryst.*, **30**, 565 (1997).

23 P. Braunstein and R. J. H. Clark, *J. Chem. Soc., Dalton Trans.*, **1973**, 1845.

24 Y. Hasegawa, M. Yamamuro, Y. Wada, N. Kanehisa, Y. Kai, and S. Yanagida, *J. Phys. Chem. A*, **107**, 1697 (2003).

25 PROCESS-AUTO; Rigaku Corporation (1996). RAXIS data-processing software. 3-9-12 Akishima, Tokyo, 196-8666, Japan.

26 ABSCOR; T. Higashi, "Empirical Absorption Correction based on Fourier Series Approximation," Rigaku Corporation, 3-9-12 Akishima, Tokyo, 196-8666, Japan, 1995.

27 SIR92; A. Altomare, G. Cascarano, C. Giacovazzo, A. Guagliardi, M. C. Burla, G. Polidori, and M. Camalli, *J. Appl. Cryst.*, **27**, 435 (1994).

28 DIRDIF94; P. T. Beurskenes, G. Admiraal, W. P. Bosman, R. de Gelder, R. Israel, and J. M. M. Smits, The DIRDIF 94 program system, Technical Report of the Crystallography laboratory, University of Nijmegen, The Netherlands, 1994.

29 TEXSAN, Version 1.11; Molecular Structure Corporation. MSC, 3200 Research Forest Drive, The Woodlands, TX 77381, USA, 2000.